Macromolecules
ARTICLE

Macromolecules **2010**, *43*, 9761–9770 **9761**
DOI: 10.1021/ma102039n

Sliding-Graft Interpenetrating Polymer Networks from Simultaneous "Click Chemistry" and Atom Transfer Radical Polymerization

Fang Yao, LiQun Xu, Guo-Dong Fu,* and BaoPing Lin*

School of Chemistry and Chemical Engineering, Southeast University, Jiangning District, Nanjing, Jiangsu Province, P.R. China 211189

Received September 2, 2010; Revised Manuscript Received November 6, 2010

ABSTRACT: In this work, a kind of semi-interpenetrating polymer network (s-IPN) with unique molecular structures, poly(ethylene glycol) (PEG) network with movable sliding-grafted poly(2-hydroxyethyl methacrylate) (PHEMA) (s-IPN-PEG/α-CD-*sg*- PHEMA), were first reported. s-IPN-PEG/α-CD-*sg*-PHEMAs were prepared by simultaneous "click chemistry" and atom transfer radical polymerization (ATRP) of a mixture of poly(ethylene glycol)-diazide/bromobutyryloxy α-cyclodextrin inclusion complex (N_3-PEG-N_3/(α-CD-BIBB)$_m$), tetrakis(2-propynyloxymethyl) methane (TMOP), CuBr, pentamethyldiethylenetriamine (PMDETA), HEMA and DMF. Attributable to the controlled characters of ATRP and the quantitative yields of "click chemistry", the prepared s-IPN-PEG/α-CD-*sg*-PHEMAs have the well-defined PEG networks, as well as uniform and tunable sliding-grafted PHEMA chains. The length of sliding-grafted PHEMA of the s-IPN-PEG/α-CD-*sg*-PHEMA can be regulated by changing polymerization times. The molecular structures, and physical and thermal properties of the s-IPN-PEG/α-CD-*sg*-PHEMA were studied by FTIR, ^{1}H NMR, XPS, TGA, and DSC measurements. The s-IPN-PEG/α-CD-*sg*-PHEMAs exhibit good physical and mechanical properties. Most important, comparing to classical semi-IPN, the diffusion of interpenetrated PHEMA from s-IPN-PEG/α-CD-*sg*-PHEMA was largely prevented for a long time solvent immersion because the PHEMA brushes were fixed on PEG networks. The sliding-grafted PHEMA chains afford functionalities to the bulk and surface of s-IPN-PEG and could potentially be used as carriers of genes and drugs.

1. Introduction

Hydrophilic interpenetrating polymer networks (HIPNs), a polymer comprising two or more networks, which are at least partially interlaced on a molecular scale but not covalently bonded to each other, have attracted much attention due to their unique properties, such as tunable responsive properties, enhanced mechanical properties, swelling characteristic, and improved thermal stability.[1−7] Thus, HIPN could be found applications as actuators and artificial muscles,[1] as sensors,[8] and in biomedical materials.[6,9−12] However, the poor mechanical properties of classical gels restrict their applications in these fields.[2] It is known that the physical properties of the HIPN were not only dominated by chemical composition, but also by their molecular structures.[13] Efforts have been made to prepare HIPNs with unique molecular structures, such as slide-ring gels,[14−16] and nanocomposite hydrogels.[17] However, the preparation of HIPNs with a well-defined and novel molecular structure is still interesting to scientists due to their unexpected properties and potential applications.

"Click chemistry", especially copper(I)-catalyzed azide−alkyne cycloaddition (CuAAC), has attracted a considerable amount of attentions for the preparation of networks due to the improved mechanical properties, complete specificity, quantitative yields and high functional group tolerance.[18−20] Hawker et al. constructed well-defined PEG networks by CuAAC.[18] The networks exhibited a surprisingly improved mechanical property in comparison to classical photochemically cross-linked PEG networks. Atom transfer radical polymerization (ATRP), a powerful tool for preparing nearly monodispersed polymers with a controllable molecular weight,[21−24] could be used to prepare networks.[25,26] However, the resulting networks exhibit poor mechanical properties. Interestingly, ATRP not only shares a number of attractive features with CuAAC, such as high tolerance toward a wide range of functional groups,[27] but also a same copper catalyst system.[28] One-pot simultaneous reaction of ATRP and CuAAC has been demonstrated by Haddleton's group[29] and used to prepare well-defined block copolymers and cross-linked nanoparticles,[30] as well as well-defined semi-IPN and full-IPN.[31]

For classical semi-IPNs (s-IPNs), the linear polymers dispersed in networks help improve the mechanical strength[32] and elasticity of polymers and bring special physical and chemical characteristics, such as temperature- or PH-sensitivity[33−35] and interfacial compatibility, to polymers.[36] However, the diffusion of linear polymers from semi-IPNs for a long time immersion in solvent, not only will reduce the physical and mechanical properties of semi-IPNs, but also limits their applications in biomedical fields.[37] Poly(ethylene glycol) (PEG) and α-cyclodextrins (α-CD) are widely studied and used as materials for biomedical,[38−42] because PEG and α-CD are biocompatible, bioabsorbable, water-soluble, and nontoxic. It is interesting that PEG was found to be included in CDs and form an inclusion complex.[43] On the basis of this property, a series of slide-ring gels with a novel molecular structure have been reported.[44−46] Here, we demonstrated a novel approach for the preparation of well-defined sliding-graft semi-IPN of PEG and poly(2-hydroxyethyl methacrylate) (s-IPN-PEG/α-CD-*sg*-PHEMAs), in which the uniform linear poly-2-hydroxyethyl methacrylate (PHEMA) was locked on the grids of PEG networks via simultaneous CuAAC and ATRP. The prepared

*To whom correspondence should be addressed: Telephone: +86-25-52090625. Fax: +86-25-52090625 E-mail: (G.-D.F.) fu7352@seu.edu.cn; (B.L.) lbp@seu.edu.cn.

Published on Web 11/17/2010

s-IPN-PEG/α-CD-*sg*-PHEMAs exhibit good physical and mechanical properties. Most important, comparing with classical semi-IPNs, the diffusion of interpenetrated PHEMAs from s-IPN-PEG/α-CD-*sg*-PHEMAs was largely prevented for a long time immersion in solvent. The sliding-grafted PHEMA chains afford functionalities to the PEG network and could be potentially used for drug or gene loading and biomedical materials with tunable functionalities on surface.

Experimental Section

1.1. Materials. The monomer 2-hydroxyethyl methacrylate (HEMA, 97%) was purchased from Acros Organic Co. of Geel, Belgium. The monomers were used after removal of inhibitors in a ready-to-use disposable inhibitors-removal column. Propargyl bromide (80%), poly(ethylene glycol) (PEG, M_n = 4000), α-cyclodextrin (α-CD), 2-bromoisobutyryl bromide (BIBB, 98%), and pentamethyldiethylenetriamine (PMDETA, 99%) were purchased from Aldrich Chemical Co. and used as received. Sodium azide (99%), CuBr (99%), methane sulfonyl chloride, pentaerythritol and other materials were purchased from Shanghai Chemical Reagent Plant.

1.2. Characterization. The chemical structures of the synthesized chemicals were characterized by ^{1}H NMR spectroscopy on a Bruker ARX 300 MHz spectrometer, using $CDCl_3$ or dimethyl sulfoxide-d_6 (DMSO-d_6) as the solvent in 1000 scans and a relaxation time of 2 s. Fourier transform infrared (FTIR) spectra were obtained from a MAGNA-IR 750 spectrometer (Nicolet Instrument Co.). The sample was dispersed in a KBr pellet. The tensile testing was performed on an Instron Model 5844 tensile testing instrument at room temperature at an extension speed of 0.01 mm/sec until the failure of the sample. The hydrogels were cut into a dumbbell shape with a length of 50 mm and width of 10 mm. The morphologies of the networks were studied by scanning electron microscope (Hitachi X-650 SEM) at an accelerating voltage of 5−20 kV and an object distance of about 8 mm. The absorption and transmittance spectra of the prepared hydrogels were measured on a Hitachi U-4100 UV−vis spectrophotometer over the 200−900 nm range with 1 nm resolution. Deionized water was used as the background correction. The hydrogels samples with a thickness of 0.5 cm were fixed on the inner wall of a quartz cell. Differential scanning calorimetry (DSC) measurement was conducted on a TA Instrument DSC Q-10 over the temperature range from −50 to +200 °C at a heating rate of 10 °C/min under nitrogen environment. DSC was calibrated with metallic indium (99.9% purity). All the prepared PEG network samples were tested in crimped aluminum pans. The thermal stability of the prepared PEG network, were carried out on a thermogravimetric analyzer (SDT-Q600, TA Instructments) at a temperature ranging from 50 to 700 °C at heating rate of 10 °C/min under nitrogen atmosphere. XPS measurements were carried out on a Kratos AXIS HSi spectrometer (Kratos Analytical Ltd., Manchester, England) with a monochromatized Al Kα X-ray source (1486.6 eV photons). The X-ray source was run at a reduced power of 150 W (15 kV and 10 mA). The samples were mounted on the standard sample studs by means of double-sided adhesive tapes. The core-level spectra were obtained at the photoelectron takeoff angle (with respect to the sample surface) of 90°. The pressure in the analysis chamber was maintained at 10^{-8} Torr or lower during sample measurements.

2.2. Chemical Synthesis. *2.2.1. Synthesis of Poly(ethylene glycol)-Diazide* (*N_3-PEG_{4K}-N_3*). Poly(ethylene glycol) diazide was prepared from PEG according to the method reported in the literature.[47] About 10 g (2.5 mmol) of PEG (M_n = 4000 g/mol) was dissolved in 50 mL dry of pyridine. The solution was cooled to 0 °C, and 0.98 g (12.5 mmol) of methanesulfonyl chloride in 10 mL of dry dichloromethane was dropwise added over 20 min. After 1 h, the reaction mixture was allowed to rise to room temperature and stirred for another 12 h. Removal of the solvent by distillation, the residue was treated with aqueous saturated $NaHCO_3$ and extracted with CH_2Cl_2. The organic solution was then dried over $MgSO_4$ for 10 h and the solvent was removed by rotary evaporation. The product was finally precipitated by addition of a large amount of diethyl ether. About 8.9 g of product was obtained. After that, a mixture of 8.0 g (2 mmol) of prepared PEG and 0.65 g (10 mmol) of sodium azide in 50 mL dry DMF was reacted at 85 °C for 24 h. The solid state was removed by passing through an alumina column, and the solution was concentrated by rotary evaporation. The polymer was precipitated from DMF concentrated solution by addition diethyl ether and filtration (yield: 90%). FTIR (cm^{-1}): $\nu_{(N=N=N)}$ = 2098. Elemental analysis indicated that the conversion from poly(ethylene glycol) to N_3-PEG_{4K}-N_3 is of about 96%.

2.2.2. Synthesis of Tetrakis(2-propynyloxymethyl)methane (*TPOM*). Tetrakis(2-propynyloxymethyl)methane (TPOM) was synthesized according to the method reported in the literature.[31] About 2.4 g (0.017 mmol) of pentaerythritol was added into a solution of 15 g (0.264 mmol) of KOH in 30 mL of anhydrous DMF. After the mixture was stirred at 5 °C for 30 min, 20 g (0.17 mmol) of propargyl bromide was slowly added over a 20 min period. The color of the solution changed to brown, and then the reaction mixture was heated at 40 °C overnight. After cooling, the reaction was quenched with water and extracted with 50 mL of ethyl ether thrice. The organic layers were combined, washed with water and then with brine, and dried over Na_2SO_4. After removal of the ethyl ether by rotary evaporation, the residue was further purified by passing a silica gel column using mixed ethyl acetate/hexanes (2/8 in volume ratio) as eluent. About 3.57 g of product was obtained (yield = 79%). ^{1}H NMR ($CDCl_3$): 4.13 (8H, $-OCHH_2$), 3.55 (8H, $C(CH_2)_4$), 2.43 (4H, CH). FTIR (cm^{-1}): $\nu_{(\equiv CH)}$ = 3299, $\nu_{(C\equiv C)}$ = 2120.

2.2.3. Synthesis of the Macroinitiator Bromobutyryloxy α-Cyclodextrin (*α-CD-BIBB*). A 250 mL round-bottom three-necked flask with a magnetic stirring bar was charged with 6.48 g (6.67×10^{-3} mol) of α-CD and kept under nitrogen before the addition of 120 mL of dry pyridine. The reaction mixture was cooled to 0 °C under stirring, a solution of 1.0 mL (8×10^{-3} mol) of 2-bromoisobutyryl bromide (BIBB) in 40 mL of $CHCl_3$ was slowly added within 30 min. Then, the reaction mixture was further stirred at room temperature for 24 h. The reaction mixtures were washed with ice water several times to remove the salt, and the organic layers were dried over anhydrous magnesium sulfate, filtered, and concentrated under reduced pressure. The obtained white solid was washed with ice water again until PH value reaches 7.0, then dried under vacuum at 50 °C to give α-CD-BIBB as a white solid. ^{1}H NMR (DMSO-d_6): 4.88 (6H, $-CH(O-)_2$, 3.35−3.9 (42H, $-OH$; $=CHO-$, $-CH_2O-$), 1.84 (6H, $-CH_3$). FTIR (cm^{-1}): $\nu_{(C=O)}$ = 1738, $\nu_{(O-H)}$ = 3369.

2.2.4. Preparation of Inclusion Complex N_3-PEG_{4K}-N_3/(α-CD-BIBB)$_m$. About 2.0 g (0.5 mmol) of poly(ethylene glycol) diazide were dissolved in 100 mL water. Then 400 mL of aqueous α-CD-BIBB solution 1.145 g (1 mmol) or 1.72 g (1.5 mmol) was added at room temperature. The mixture was ultrasonically agitated for 30 min and then allowed to stand overnight. The white precipitate was collected by centrifugation, washed with ice water, then dried under vacuum at 70 °C to give α-CD-BIBB and N_3-PEG_{4K}-N_3 inclusion complex (N_3-$PEG_{4K}N_3$/(α-CD-BIBB)$_m$, m = 1.1 or 2.3). FTIR (cm^{-1}): $\nu_{(C=O)}$ = 1738, $\nu_{(O-H)}$ = 3413.

2.2.5. Preparation of s-IPN-PEG/α-CD-sg-PHEMAs from Simultaneous CuAAC and ATRP. A typical procedure for preparation of s-IPN-PEG/α-CD-*sg*-PHEMAs via simultaneous ATRP of HEMA and "click chemistry" of inclusion complex N_3-PEG_{4K}-N_3/(α-CD-BIBB)m with tetrakis(2-propynyloxymethyl)methane was briefly described as follows. 2.64 mL (22 mmol) of HEMA, 29 mg (0.2 mmol) of CuBr, 0.52 g (0.1 mmol) of inclusion complex N_3-PEG_{4K}-N_3/(α-CD-BIBB)$_{1.1}$, 14.4 mg (0.05 mmol) of tetrakis(2-propynyloxymethyl)methane and 1.5 mL of DMF were introduced into a small vial. After 20 min of argon

Scheme 1. Process of the Preparation of Poly(ethylene glycol) (PEG, M_n = 4000 g/mol) Network with Movable Sliding-Graft Poly(2-hydroxyethyl methacrylate) (PHEMA) (s-IPN-PEG/α-CD-*sg*-PHEMA) via Simultaneous ATRP and "Click Chemistry" (CuAAC)

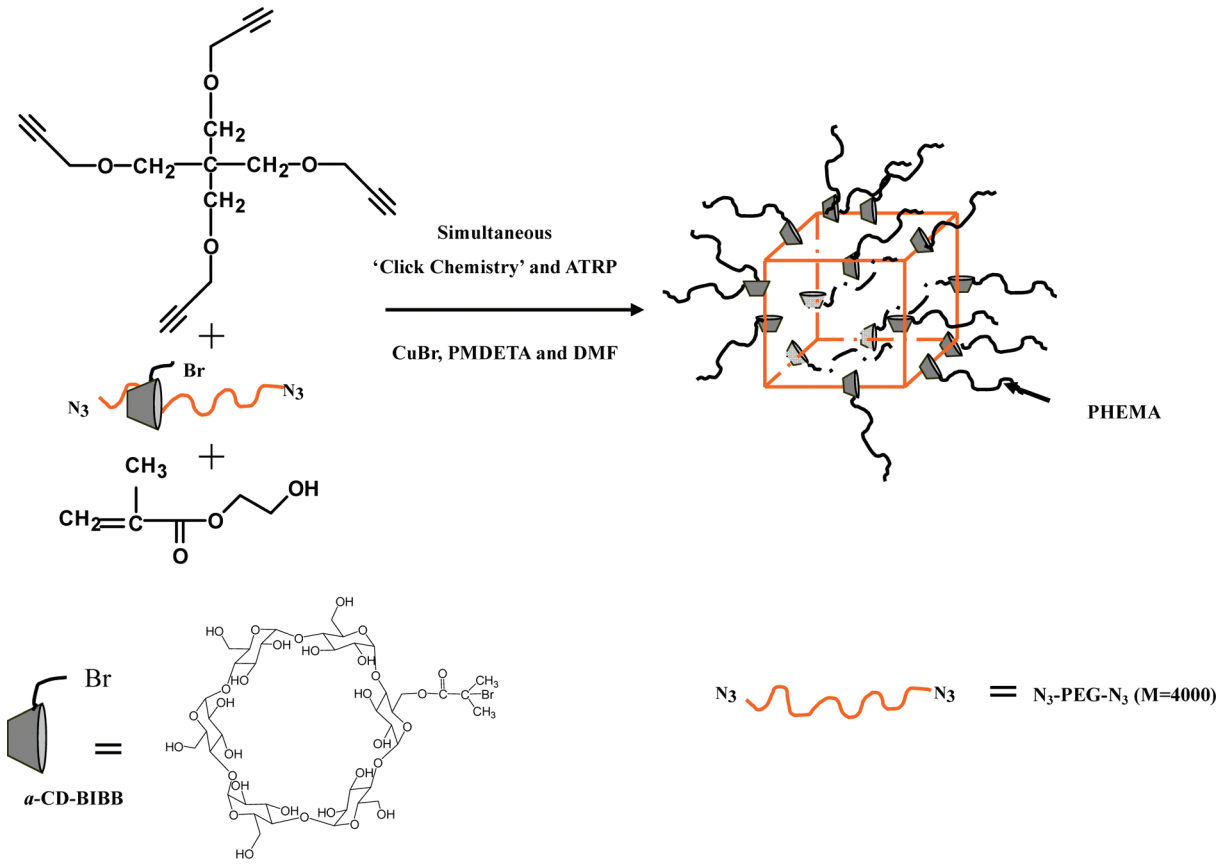

degassing, PMDETA [42 uL (0.2 mmol)] was added to the flask with a syringe under ultrasonic agitation (the ratio of reagents $[N_3\text{-}PEG_{4K}\text{-}N_3/(\alpha\text{-CD-BIBB})_{1.1}]$:[TOPM]:[CuBr]:[PMDETA]:[HEMA] = 0.5:0.25:1:1:110). The gelation of reaction occurs in 2 min. The mixture was kept at 60 °C for a predetermined period of time to obtain the uniform solid semi-IPN. A uniform s-IPN was obtained upon removal from the vial. The prepared s-IPN-PEG/α-CD-*sg*-PHEMA was transferred to an EDTA (5%) solution to remove the copper ions and DMF. Finally, the s-IPN-PEG/α-CD-*sg*-PHEMA was immersed into a large volume of pure deionized water to allow the maximum water absorption.

2.2.6. Preparation of Pristine PEG Network from CuAAC. About 0.1 g (0.025 mmol) of poly(ethylene glycol) diazide ($N_3\text{-}PEG_{4K}\text{-}N_3$), 3.6 mg (0.0125 mmol) of tetrakis(2-propynyloxymethyl)methane, 8.7 mg (0.05 mmol) of PMDETA, and 1 mL of DMF were introduced into a small vial. After the mixture turned clear, the vial was degassed with argon for 20 min, and 7.2 mg (0.05 mmol) of CuBr was quickly added under ultrasonic agitation. The gelation point was reached in 1 min, and the reaction was allowed to continue to a predetermined period of time at 60 °C. A uniform PEG network was obtained upon removal from the vial. The prepared network was transferred to an EDTA (5%) solution to remove the copper ions and DMF. Finally, the PEG network was immersed into a large volume of pure deionized water to allow the maximum water absorption.

2.2.7. Preparation of Slide-Ring PEG/(α-CD-BIBB)$_m$ Network from CuAAC. A typical procedure for preparation of slide-ring PEG/α-CD network via "click chemistry" as follows. A 29 mg (0.2 mmol) sample of CuBr, 0.52 g (0.1 mmol) of inclusion complex $N_3\text{-}PEG_{4K}\text{-}N_3/(\alpha\text{-CD-BIBB})_{1.1}$, 14.4 mg (0.05 mmol) of tetrakis(2-propynyloxymethyl)methane, and 1.5 mL of DMF were introduced into a small vial. After 20 min of argon degass, 42 uL (0.2 mmol) of PMDETA was added to the flask with a syringe under ultrasonic agitation (The ratio of reagents $[N_3\text{-}PEG_{4K}\text{-}N_3/(\alpha\text{-CD-BIBB})_{1.1}]$:[TOPM]:[CuBr]:[PMDETA] = 0.5:0.25:1:1:1). The gelation of reaction occurs in 90 s. The mixtures were kept at 60 °C for a predetermined time to obtain a solid uniform gel. The PEG network was transferred to an EDTA (5%) solution to remove the copper ions and DMF. Finally, the PEG network was immersed into a large volume of pure deionized water to allow the water absorption.

2.2.8. Preparation of s-IPN-PEG/PHEMA via Simultaneous CuAAC and ATRP. Typical s-IPN of PEG/PHEMA was prepared via simultaneous ATRP of HEMA and "click chemistry" of $N_3\text{-}PEG_{4K}\text{-}N_3$ with TPOM was briefly described as follows. 2.64 mL (22 mmol) of HEMA, 29 mg (0.2 mmol) of CuBr, 0.4 g (0.1 mmol) of $N_3\text{-}PEG_{4K}\text{-}N_3$, 14.4 mg (0.05 mmol) of tetrakis(2-propynyloxymethyl)methane, 29.4 uL (0.2 mmol) of ethyl α-bromobutyrate (EBB), and 1.5 mL of DMF were introduced into a small vial. After 20 min of argon degass, 42 μL (0.2 mmol) of PMDETA was added to the flask with a syringe under ultrasonic agitation (the ratio of reagents $[N_3\text{-}PEG_{4K}\text{-}N_3]$:[TOPM]:[EBB]:[CuBr]:[PMDETA]:[HEMA] = 0.5:0.25:1:1:1:110). The gelation of s-IPN occurred in 2 min. The mixture was kept at 60 °C for a predetermined time to obtain the uniform solid s-IPN. The copper catalyst and DMF in the s-IPN were also removed in 5% EDTA solution, and maximum water absorption was achieved by immersing the s-IPN in deionized water.

2.2.9. Swelling Ratio. Swelling behavior of the prepared PEG networks was studied by a gravimetric method. Dry films were immersed in distilled water at 25 °C, and the swollen weight was measured for each sample at a given time after excess surface water was blotted carefully with moistened filter paper. The value was recorded until the weights do not increase further. The swelling ratio (SR) of PEG networks were determined gravimetrically using following relation:

$$\mathrm{SR} = [(m_t - m_0)/m_0] \times 100\%$$

Here m_t is the mass of the swollen hydrogels at time t and m_0 is the mass of the dry gel. Each value was the average value from five measurements.

2.2.10. Water Extraction. The prepared semi-IPN were initially dried at 50 °C in vacuum more than 24 h until sample weight reached a constant value, and the weight was recorded as W_0. Then the dried semi-IPN sample was immersed in water for predetermined time to allow linear PHEMA diffuse into water. Afterward, sample was collected out of water and dried at 50 °C in vacuum until sample weight reached a constant value, and the weight was recorded again as W_t, where t is immersion time. Weight percent = W_0/W_t. Each value was the average value from five measurements.

3. Results and Discussions

3.1. Synthesis of Sliding-Graft Semi-IPN of PEG and PHEMA (s-IPN-PEG/α-CD-*sg*-PHEMAs) via Simultaneous ATRP and CuAAC. Scheme 1 shows the preparation of the sliding-graft semi-IPN of PEG and PHEMA (s-IPN-PEG/α-CD-*sg*-PHEMA) from simultaneous CuAAC and ATRP. s-IPN-PEG/α-CD-*sg*-PHEMA was prepared from the one-pot simultaneous reactions of (1) "click chemistry" (CuAAC) of the poly(ethylene glycol) diazide (M_n = 4000 g/mol, N_3-PEG_{4K}-N_3) and α-CD-BIBB inclusion complex initiators (N_3-PEG_{4K}-N_3/(α-CD-BIBB)$_m$) and tetrakis(2-propynyloxymethyl)methane (TPOM) to generate the network with 1,2,3-triazole linkages and (2) ATRP of 2-hydroxyethyl methaycrylate (HEMA) using N_3-PEG_{4K}-N_3/(α-CD-BIBB)$_m$ as initiator, copper(I) bromide as catalyst and pentamethyldiethylenetriamine (PMDETA) as ligand. Here N_3-PEG_{4K}-N_3/(α-CD-BIBB)$_m$ not only serves as reaction agents for "click chemistry", but also acts as the initiators for ATRP of HEMA.

First, the ATRP initiator of α-CD-BIBB was synthesized. The successful preparation of α-CD-BIBB was confirmed by FTIR with characteristic absorption peak of ester group at 1738 cm^{-1}. Calculating from ^1H NMR results of α-CD-BIBB with the integral areas of peak at 1.84 ppm (CH_3) and peak at 4.88 ppm((-O)$_2$CH−), each α-CD-BIBB has about of 1.12 initiating sites. Then, α-CD-BIBB were threaded onto poly(ethylene glycol)-diazide (N_3-PEG_{4K}-N_3) chains to prepare N_3-PEG_{4K}-N_3/(α-CD-BIBB)$_m$. The formation of inclusion complex was studied by FTIR characterization. The α-CD-BIBB shows an extremely strong absorption band at 3369 cm^{-1}, which is attributable to the symmetric and asymmetric O−H stretching mode. The shift of broad O−H band to 3413 cm^{-1}, due to the noncovalent interaction between O−H of α-CD and the N_3-PEG_{4K}-N_3 macromolecules, reveals that the N_3-PEG_{4K}-N_3 and α-CD-BIBB inclusion complex is formed by host and guest interaction.[48] The number of α-CD-BIBB in inclusion complex can be readily tuned by changing the α-CD-BIBB and N_3-PEG_{4K}-N_3 feed ratio. The number of α-CD-BIBB in each N_3-PEG_{4K}-N_3/(α-CD-BIBB)$_m$ inclusion complex can be calculated from ^1H NMR results, using the integral areas of peak at 4.88 ppm ((-O)$_2$CH−), assigned to character protons of α-CD-BIBB, and peak in the range of 3.2−4.0 ppm ((−OCH$_2$CH$_2$−) attributable to N_3-PEG_{4K}-N_3 protons. Here, N_3-PEG_{4K}-N_3/(α-CD-BIBB)$_m$ inclusion complexes, having average 1.1 of α-CD-BIBB (N_3-PEG_{4K}-N_3/(α-CD-BIBB)$_{1.1}$, m = 1.1) and 2.3 of α-CD-BIBB (N_3-PEG_{4K}-N_3/(α-CD-BIBB)$_{2.3}$, m = 2.3) on each N_3-PEG_{4K}-N_3, were prepared.

Sliding-graft semi-IPN of PEG and PHEMA (s-IPN-PEG/α-CD-*sg*-PHEMA) was prepared via simultaneous CuAAC and ATRP from a reaction mixture of N_3-PEG_{4K}-N_3/(α-CD-BIBB)$_m$, TPOM, CuBr, PMDETA, HEMA and DMF. Slide-ring PEG/(α-CD-BIBB)$_m$ networks were prepared via CuAAC with a the same reaction condition as that for the preparation of s-IPN-PEG/α-CD-*sg*-PHEMAs albeit in the absence of HEMA. Figure 1 shows the optical images (a) of the pristine PEG network from CuAAC, (b) of slide-ring PEG/(α-CD-BIBB)$_{1.1}$ from CuAAC, and (c) of the s-IPN-PEG/α-$CD_{1.1}$-*sg*-$PHEMA_{51}$ via simultaneous CuAAC and ATRP (in Table 1), respectively.

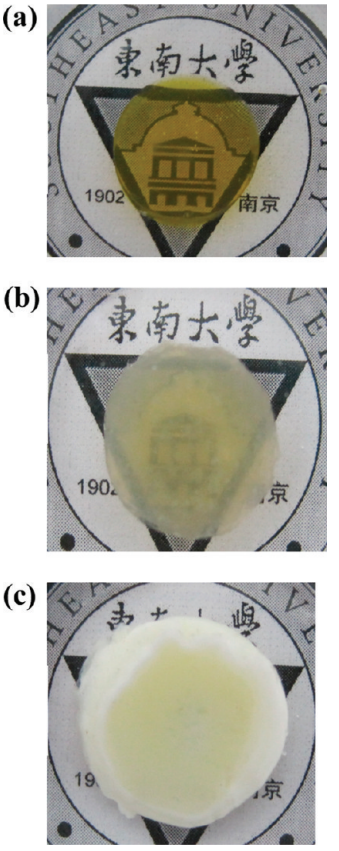

Figure 1. Photographs (a) of the pristine PEG hydrogel from "click chemistry" (CuAAC), (b) of slide-ring PEG/(α-CD-BIBB)$_{1.1}$ hydrogel from "click chemistry" (CuAAC), and (c) of the s-IPN-PEG/α-$CD_{1.1}$-*sg*-$PHEMA_{51}$ hydrogel via simultaneous "click chemistry" (CuAAC) and ATRP (in Table 1), respectively.

Since CuAAC and ATRP share a same catalyst system, the concentration of Cu(I) catalyst plays an important role in the gelation effect. Previous work[31] shows, the increase in the amount of Cu(I) catalyst can reduce the gelation time. In this study, N_3-PEG_{4K}-N_3/(α-CD-BIBB)$_{1.1}$ inclusion complex was used for the preparation of s-IPN-PEG/α-$CD_{1.1}$-*sg*-PHEMAs. By increasing the concentration of CuBr from 25% to 200% (relative to the mole concentration of azido and alkynyl groups), the respective gelation time decreased from about 30 min to 20 s. In this study, s-IPN-PEG/α-$CD_{1.1}$-*sg*-PHEMAs were prepared with an [N_3-PEG-N_3/(α-CD-BIBB)$_{1.1}$]:[TPOM]:[HEMA]:[CuBr]:[PMDETA] molar ratio of 0.5:0.25:110:1:1. The gelation was reached in 2 min. The disappearance of FTIR absorption band at 2080 cm^{-1} assigned to azide group and at 2120 cm^{-1} assigned to alkynyl group, as well as the appearance of the strong broad absorption band at 3360 cm^{-1} attributed to the hydroxyl group of PHEMA, suggested that the s-IPN-PEG/α-CD-*sg*-PHEMAs was prepared. The successful preparation of s-IPN-PEG/α-CD-*sg*-PHEMAs was also confirmed by X-ray photoelectron spectroscopy (XPS). Figure 2 shows the XPS C 1s core-level spectra (a) of the pristine PEG network, (b) of slide-ring PEG/(α-CD-BIBB)$_{1.1}$ network, and (c) of sliding-graft

Table 1. Characterization of sliding-graft semi-interpenetrating networks

sample	molar feed ratio [N_3-PEG-N_3/(α-CD-BIBB)$_m$]:[TOPM]:[CuBr]:[PMDETA]:[HEMA]:[DMF]	polymerization time (h)	gel fraction (%)	HEMA conversion	sol−gel fraction[b][PEG/(α-CD]:[PHEMA]:[water] (%)		SR[i](%)	max. stress[j] (kPa)	max. extension to break[j]
					after EDTA extraction	after water extraction[i]			
pristine PEG network[a]		6	0.94	0			1570 ± 110	630 ± 17	800 ± 59
slide-ring PEG/(α-CD-BIBB)$_{1.1}$[b]	0.5:0.25:1: 1: 0:97	6	0.90	0	11:0:89	11:0:89	820 ± 80	620 ± 23	400 ± 27
slide-ring PEG/(α-CD-BIBB)$_{2.3}$[b]	0.5:0.25:1: 1: 0:97	6	0.84	0	15:0:85	15:0:85	660 ± 60	600 ± 31	360 ± 30
s-IPN-PEG/α-CD$_{1.1}$-*sg*-PHEMA$_{23}$[b]	0.5:0.25:1:1:110:97	6	0.90[d]	0.23[f]	12:7:81	12:7:81	520 ± 85	980 ± 26	320 ± 50
s-IPN-PEG/α-CD$_{1.1}$-*sg*-PHEMA$_{35}$[b]	0.5:0.25:1:1:110:97	12	0.90[d]	0.35[f]	14:13:73	14:13:73	370 ± 70	990 ± 40	300 ± 65
s-IPN-PEG/α-CD$_{1.1}$-*sg*-PHEMA$_{51}$[b]	0.5:0.25:1:1:110:97	24	0.90[d]	0.51[f]	13:18:69	13:28:69	320 ± 80	1050 ± 32	270 ± 42
s-IPN-PEG/α-CD$_{2.3}$-*sg*-PHEMA$_{19}$[b]	0.5:0.25:1:1:230:97	6	0.84[e]	0.19[f]	16.5:12.5:71	16.5:12.5:71	340 ± 90	930 ± 45	340 ± 35
s-IPN-PEG/PHEMA[c]		24	0.90	0.74[g]	2.7:6.3:91	2.8:5.9:91.3	1050 ± 30	640 + 30	600 ± 40

[a] Molar feed ratio of [N_3-PEG-N_3]:[TOPM]:[CuBr]:[PMDETA] = 0.5:0.25:1:1, the reaction was carried at 60 °C. [b] The reaction was carried at 60 °C. [c] Molar feed ratio of [N_3-PEG$_{4K}$-N_3]:[TOPM]:[EBB]:[CuBr]:[PMDETA]:[HEMA] = 0.5:0.25:1:1:1:110, the reaction was carried at 60 °C. [d] It was assumed that the s-IPN-PEG/α-CD$_{1.1}$-*sg*-PHEMA gels have a same gel fraction as that of corresponding slide-ring PEG/(α-CD-BIBB)$_{1.1}$. [e] It was assumed that the s-IPN-PEG/α-CD$_{2.3}$-*sg*-PHEMA gels have a same gel fraction as that of corresponding slide-ring PEG/(α-CD-BIBB)$_{2.3}$. [f] The HEMA conversion calculated from an equation of [Mass$_{\text{dried-gel of s-IPN-PEG/α-CD-}sg\text{-PHEMA}}$ − Mass$_{\text{dried sliding-ring PEG/(α-CD-BIBB)}m\text{ gel}}$]/Mass$_{\text{HEMA}}$. [g] The HEMA conversion calculated from an equation of [Mass$_{\text{dried-gel of s-IPN-PEG/PHEMA}}$ − Mass $_{\text{PEG gel}}$]/Mass$_{\text{HEMA}}$. [h] The sol−gel fractions were calculated from the data of SR, gel-fraction and HEMA conversion. [i] The time of water extraction is 20 h. [j] The value is the average of five measurements.

Scheme 2. Theoretical Molecular Structures (a) of Pristine PEG Network from "Click Chemistry" (CuAAC), (b) of Slide-Ring PEG/(α-CD-BIBB)$_m$ from "Click Chemistry" (CuAAC) and (c) of s-IPN-PEG/α-CD-*sg*-PHEMA via Simultaneous "Click Chemistry" (CuAAC) and ATRP

s-IPN-PEG/α-CD-*sg*-PHEMAs (s-IPN-PEG/α-CD$_{1.1}$-*sg*-PHEMA$_{23}$ in Table 1), respectively. For pristine PEG network from CuAAC, it has only one peak component at 286.2 eV, which is attributable to *C*-O and *C*-*N*= species.[49] The C 1s core-level spectrum of slide-ring PEG/(α-CD-BIBB)$_{1.1}$ network can be curve-fitted into four peak components with bonding energy (BEs) at about 284.6 eV, 286.2 eV, 287.6 and 288.4 eV, attributable to *C*−H/*C*−C, C−O/*C*−Br, O−*C*−O, and O−*C*═O species, respectively. Since *a*-CD-BIBB is water-soluble, unthreaded *a*-CD-BIBB on gel surface would be removed by long time water immersion. Thus, the presence of peak components at 287.6 and 288.4 eV, associated with the *a*-CD and bromide-capped ester group of *a*-CD-BIBB, reveals that slide-ring PEG/(*a*-CD-BIBB)$_m$ network has been successfully prepared. In Figure 2c, the increase in intensity of C−H/C−C and O−C═O species is consistent with the appearance of the poly(2-hydroxyethyl methacrylate) (PHEMA) brushes in s-IPN-PEG/α-CD$_m$-*sg*-PHEMAs. Scheme 2 shows the possible molecular structures (a) of the pristine PEG network, (b) of slide-ring PEG/(α-CD-BIBB)$_m$ network, and (c) of sliding graft sliding graft s-IPN-PEG/α-CD$_m$-*sg*-PHEMAs, respectively. XPS results consist with the molecular structures of the corresponding networks.

The gel fraction of the s-IPN-PEG/α-CD$_m$-*sg*-PHEMAs is one of the main concerns. The data in Table 1 show that gel fraction of pristine PEG network, slide-ring PEG/(*a*-CD-BIBB)$_m$ and sliding graft s-IPN-PEG/α-CD$_m$-*sg*-PHEMA. The gel fraction was obtained from the expression: Gel fraction = Mass$_{\text{dried-gel}}$/Mass$_{\text{polymer-precursors}}$. The gel fraction of

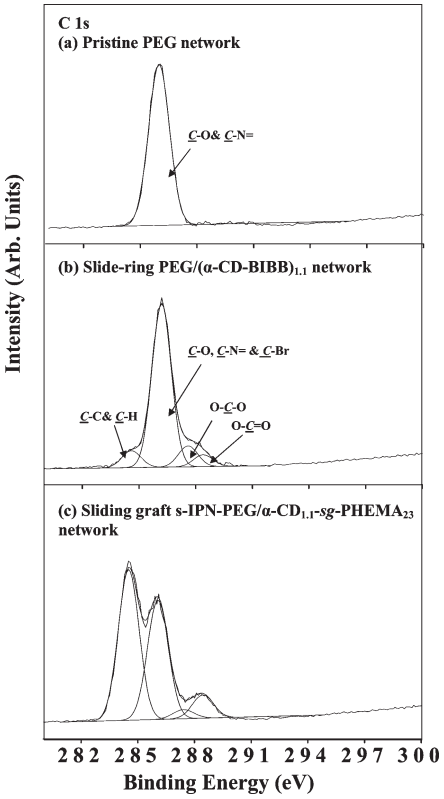

Figure 2. X-ray photoelectron spectroscopy (XPS) C 1s core-level spectra (a) of the pristine PEG networks, (b) of slide-ring PEG/(α-CD-BIBB)$_{1.1}$ network, and (c) of s-IPN-PEG/α-CD-*sg*-PHEMAs (s-IPN-PEG/α-CD$_{1.1}$-*sg*-PHEMA$_{23}$) network in Table 1, respectively.

slide-ring PEG/(α-CD-BIBB)$_{1.1}$ network was about 90%, which was slightly lower than that (94%) of pristine PEG network, while is higher than that (84%) of slide-ring PEG/(α-CD-BIBB)$_{2.3}$ networks. The gel fraction decreases with increase in the number of α-CD-BIBB in N_3-PEG$_{4K}$-N_3/(α-CD-BIBB)$_m$. This could be accounted for the facts that the inclusion of the α-CD-BIBB enhances the rigid of the PEG chain and reduces the molar free volume of polymer chains, which reduced the efficiency of "click chemistry". The length of PHEMA brushes of s-IPN-PEG/α-CD$_m$-*sg*-PHEMAs can be calculated from the conversion of HEMA monomers. The conversion of HEMA was calculated from the expression of [Mass$_{\text{dried-gel of s-IPN-PEG/α-CDm-}sg\text{-PHEMA}}$ − Mass$_{\text{dried sliding-ring PEG/(α-CD-BIBB)m gel}}$]/Mass$_{\text{HEMA}}$. The data in Table 1 indicate that, at a reaction time of 6 h, the conversion of HEMA is of about 0.23, that is, the theoretical length of PHEMA on α-CD-BIBB is about of 23. The length of PHEMA brushes can be regulated by polymerization time. Table 1 also shows, with the polymerization time increase from 6 to 12 and 24 h, the conversion of HEMA enhanced from 23% to 35% and 51%, respectively. Correspondingly, the length of PHEMA brushes on α-CD-BIBB increases from 23 to 35 and 51 repeat units. In fact, the rate of "click chemistry" was very fast. In the process of simultaneous "click chemistry"(CuAAC) and ATRP, about 90% of Click conversion can be achieved in 5 min.[29] Thus, in the first few minutes, "click chemistry" was the predominant reaction. With process of reactions and completion of the Click reaction, ATRP of HEMA became dominated reaction. At this stage, the polymerization may be considered as the ATRP of HEMA in a PEG-based network. Previous works[31] indicated that after 30 min, extending reaction time just increases the conversion of ATRP, but the PEG gel fraction can not be improved further.

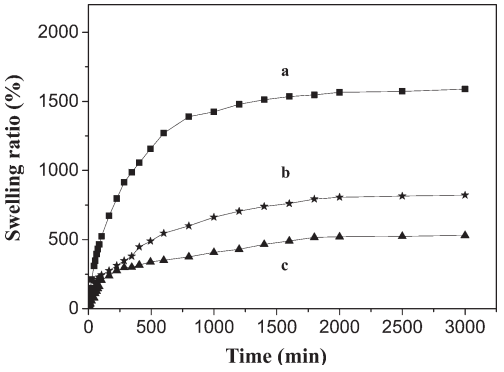

Figure 3. Swelling ratio in deionized water of (a) pristine PEG hydrogel from "click chemistry" (CuAAC), (b) of slide-ring PEG/(α-CD-BIBB)$_{1.1}$ hydrogel from "click chemistry" (CuAAC), and (c) of s-IPN-PEG/α-CD$_{1.1}$-*sg*-PHEMA$_{23}$ via simultaneous "click chemistry" (CuAAC) and ATRP (in Table 1) as a function of time.

3.2. Swelling and Transmittance Performance. Figure 3 shows the degree of swelling ratio (SR) of (a) pristine PEG network, (b) of slide-ring PEG/(α-CD-BIBB)$_{1.1}$, and (c) of s-IPN-PEG/α-CD$_{1.1}$-*sg*-PHEMA$_{23}$ as a function of time. As shown, all samples can reach swelling degree of 80% in 500 min. Pristine PEG network from CuAAC exhibit a swelling degree of about 1570%, which is much higher than that (820%) of slide-ring PEG/(α-CD-BIBB)$_{1.1}$ and that (520%) of s-IPN-PEG/α-CD$_{1.1}$-*sg*-PHEMA$_{23}$. The increase in the number of α-CD-BIBB thread on PEG chain[50] and the length of PHEMA also leads to the reduction of swelling degree of hydrogels. The data in Table 1 show, the slide-ring PEG/(α-CD-BIBB) $_{2.3}$ hydrogel has a swelling degree of about 660%, which is much low than that of slide-ring PEG/(α-CD-BIBB)$_{1.1}$ hydrogel. The swelling degree of s-IPN-PEG/α-CD$_{1.1}$-*sg*-PHEMA$_{51}$ is about of 320%, which is lower than that (370%) of s-IPN-PEG/α-CD$_{1.1}$-*sg*-PHEMA$_{35}$ and that (520%) of s-IPN-PEG/α-CD$_{1.1}$-*sg*-PHEMA$_{23}$. This could be accounted for the facts as follows: (1) the networks from "click chemistry" are well-defined and the maximum SR of PEG network are dominated by the size of network lattice, that is the chain length of PEG. Since the networks are made from PEG$_{4K}$, thus the theoretic free volume of hydrogels are same; (2) the inclusion of the α-CD-BIBB and the sliding-grafted α-CD-*sg*-PHEMA chains would reduce the free volume of the PEG network lattices; (3) moreover, the interaction of the α-CD-BIBB and entanglement of the sliding-grafted α-CD-*sg*-PHEMA chains restrict the full stretching of the network lattices and resulting in a lower degree of swelling; (4)The decrease in the swelling degree of s-IPN-PEG/α-CD-*sg*-PHEMA with a high PHEMA composition could also be accounted for the fact that PHEMA is a relatively more hydrophobic than PEG. Figure 4 shows the scanning electron microscopy (SEM) cross-sectional images of the freeze-dried samples (a) of the pristine PEG network, (b) of slide-ring PEG/(α-CD-BIBB)$_{1.1}$ and (c) of s-IPN-PEG/α-CD$_{1.1}$-*sg*-PHEMA$_{51}$ networks. As shown in Figure 4a, the pristine PEG network is highly porous with pore sizes ranging from 40 to 120 μm. While s-IPN-PEG/α-CD$_{1.1}$-*sg*-PHEMA$_{51}$ has a homogeneous and dense morphology. The morphologies reveal the sliding-grafted α-CD$_m$-*sg*-PHEMAs chains take up the space volume between the lattices of PEG networks, thus leading to a low swelling degree in s-IPN-PEG/α-CD-*sg*-PHEMAs. The SEM results are consistent with the swelling ratio, that is, the more porous the structure, the higher the degree of swelling.

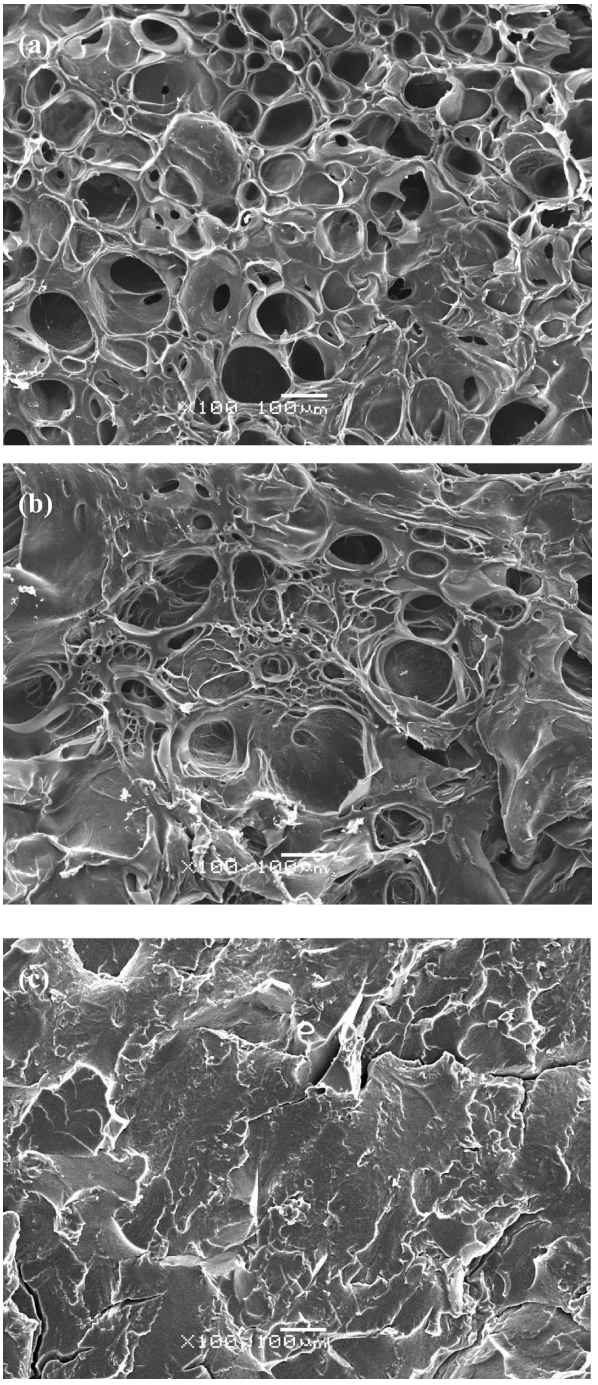

Figure 4. Scanning electron microscopy (SEM) cross-sectional views of the freeze-dried samples (a) of the pristine PEG network, (b) of slide-ring PEG/(α-CD-BIBB)$_{1.1}$ and (c) of s-IPN-PEG/α-CD$_{1.1}$-*sg*-PHEMA$_{51}$ networks.

One of the possible plausible applications of s-IPN is used as soft contact lenses. The optic property of s-IPN-PEG/α-CD-*sg*-PHEMA is another concern. Figure 5 shows the transmittance (a) of the pristine PEG hydrogel, (b) of slide-ring PEG/(α-CD-BIBB)$_{1.1}$ and (c) of s-IPN-PEG/α-CD$_{1.1}$-*sg*-PHEMA$_{51}$ hydrogels. The pristine PEG hydrogel has a higher transmittance than those of slide-ring PEG/(α-CD-BIBB)$_{1.1}$ and s-IPN-PEG/α-CD$_{1.1}$-*sg*-PHEMA$_{51}$ hydrogels. The slide-ring PEG/(α-CD-BIBB)$_{1.1}$ hydrogel and s-IPN-PEG/α-CD$_{1.1}$-*sg*-PHEMA$_{51}$ hydrogel exhibit a high UV resistance. In the range of 200 to 300 nm, the transmittance of slide-ring PEG/(α-CD-BIBB)$_{1.1}$ and s-IPN-PEG/α-CD$_{1.1}$-*sg*-PHEMA$_{51}$

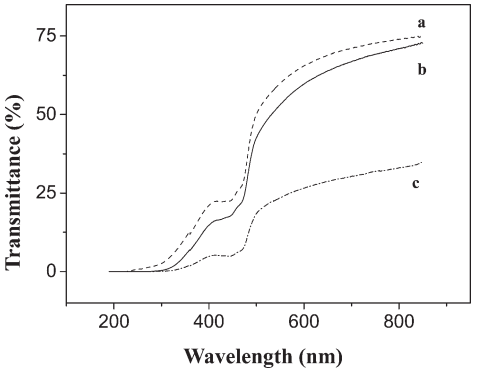

Figure 5. UV−visible transmittance spectra (a) of the pristine PEG hydrogel, (b) of slide-ring PEG/(α-CD-BIBB)$_{1.1}$, and (c) of s-IPN-PEG/α-CD$_{1.1}$-*sg*-PHEMA$_{51}$ hydrogels.

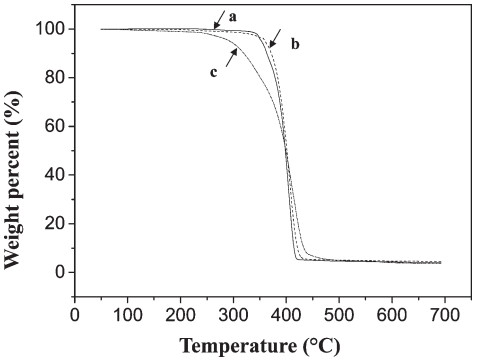

Figure 6. Thermogravimetric analysis (TGA) curves (a) of pristine PEG network, (b) of slide-ring PEG/(α-CD-BIBB)$_{1.1}$, and (c) of s-IPN-PEG/α-CD$_{1.1}$-*sg*-PHEMA$_{51}$ networks.

hydrogels is lower less than 1%. At the wavelength of 400 nm, the transmittance of s-IPN-PEG/α-CD$_{1.1}$-*sg*-PHEMA$_{51}$ hydrogel is about 4.9%, which is lower than that (15.2%) of slide-ring PEG/(α-CD-BIBB)$_{1.1}$ and that (21.6%) of pristine PEG hydrogels. The good UV-resistance of s-IPN-PEG/α-CD-*sg*-PHEMAs may attribute to the UV absorption of PEG and PHEMA polymers,[51] as well as the reflection at interfaces and scattering due to the phase separation. In the visible region, the transmittance of hydrogels increases with the increase in the wavelength. The pristine PEG hydrogel and slide-ring PEG/(α-CD-BIBB)$_{1.1}$ exhibit a high transparence. At the wavelength of 800 nm, the transmittance of the slide-ring PEG/(α-CD-BIBB)$_{1.1}$ hydrogel is about of 71%, which is very close to that (75%) of pristine PEG hydrogel. The presence of sliding-grafted α-CD-*sg*-PHEMA in s-IPN-PEG/α-CD-*sg*-PHEMA hydrogel largely reduces the transparence. For the s-IPN-PEG/α-CD$_{1.1}$-*sg*-PHEMA$_{51}$ hydrogel, the transmittance is less than 35% at 800 nm. The low transmittance of s-IPN-PEG/α-CD-*sg*-PHEMA could be attributable to the phase separation between the PEG network and sliding-grafted α-CD-*sg*-PHEMA chains.

3.3. Thermal and Mechanical Properties. The thermal stability is very important for materials aiming for biomedical applications. Here the thermal properties of s-IPN-PEG/α-CD-*sg*-PHEMA were studied by TGA and DSC. Figure 6 shows the thermalgravimetric analysis (TGA) curves of dried pristine PEG network, slide-ring PEG/(α-CD-BIBB)$_{1.1}$ and s-IPN-PEG/α-CD$_{1.1}$-*sg*-PHEMA$_{51}$ networks. It shows three different decomposition temperatures (T_d) at about 337, 359, and 237 °C for pristine PEG network, slide-ring PEG/(α-CD-BIBB)$_{1.1}$ and s-IPN-PEG/α-CD$_{1.1}$-*sg*-PHEMA$_{51}$ networks, respectively. The slide-ring PEG/(α-CD-BIBB)$_{1.1}$

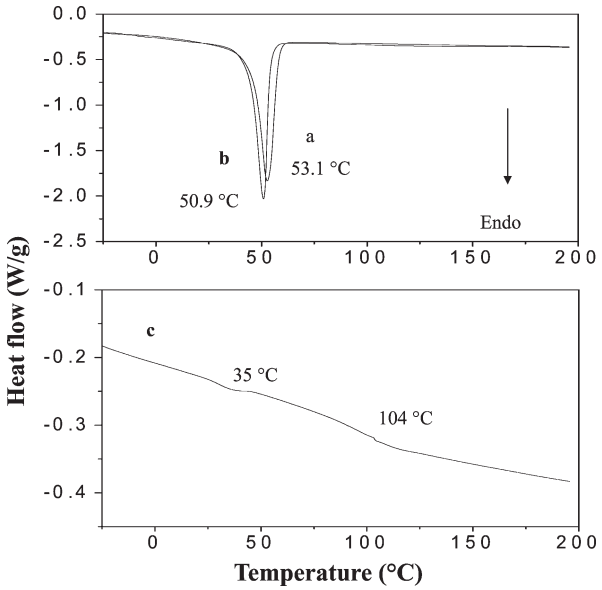

Figure 7. Differential scanning calorimetry (DSC) curves of dried (a) pristine PEG network, (b) slide-ring PEG/(α-CD-BIBB)$_{1.1}$, and (c) s-IPN-PEG/α-CD$_{1.1}$-*sg*-PHEMA$_{51}$ networks.

networks undergoes thermal decomposition at 359 °C, which is higher than that (337 °C) of pristine PEG network. The PEG/α-CD inclusion complex exhibits a high thermal stability than both PEG and α-CD chemicals.[52] Thus, the increase in thermal stability suggests that the slide-ring PEG/(α-CD-BIBB)$_m$ have been successfully prepared. The weight loss of s-IPN-PEG/α-CD-*sg*-PHEMA commences at 237 °C, which is much lower than that of pristine PEG network and slide-ring PEG/(α-CD-BIBB)$_m$. The presence of the easily decomposable composition (sliding-grafted α-CD-*sg*-PHEMA) reduces the thermal stability of the s-IPN-PEG/α-CD-*sg*-PHEMA networks.

Figure 7 shows the differential scanning calorimetry (DSC) curves (a) of pristine PEG network, (b) of slide-ring PEG/(α-CD-BIBB)$_{1.1}$ and (c) of s-IPN-PEG/α-CD$_{1.1}$-*sg*-PHEMA$_{51}$ networks, respectively. The melting transition temperature (T_m) of slide-ring PEG/(α-CD-BIBB)$_{1.1}$ network is of about 50.9 °C, which is lower than that (53.1 °C) of pristine PEG network. The threaded α-CD onto the lattice of PEG network both destroys the ordered molecular structure and decreases the mobility of PEG. Thus, the decrease in T_m also suggests that the slide-ring PEG/(α-CD-BIBB)$_m$ networks have been successfully prepared. There were two transitions in the DSC curves of s-IPN-PEG/α-CD-*sg*-PHEMA. The first weak endothermic peak appeared at around 35 °C is associated with the melting temperature (T_m) of the PEG network. The second endothermic peak at around 104 °C is attributable to the glass transition temperature (T_g) of PHEMA. The decrease in the T_m of PEG network in s-IPN-PEG/α-CD-*sg*-PHEMA can be accounted that the appearance of sliding-graft α-CD-*sg*-PHEMA largely reduced the crystallinity of PEG networks. The decrease of the crystallinity of PEG networks in s-IPN-PEG/α-CD-*sg*-PHEMA was also revealed by the reduction of melting enthalpy. The melting enthalpy of a 100% crystalline PEG (MW = 4000) is 51.5 cal/g (214.6 J/g).[53] The melting enthalpy of the pristine PEG networks from CuAAC is about of 22.1 J/g (crystallinity = 10.3%), which is higher than 15.2 J/g (crystallinity = 7.1%) of slide-ring PEG/(α-CD-BIBB)$_{1.1}$ network and higher than 0.34 J/g (crystallinity = 0.16%) of s-IPN-PEG/α-CD$_{1.1}$-*sg*-PHEMA$_{51}$ network.

All prepared hydrogels exhibit a good mechanical property, in comparison to the classic hydrogels.[32] In comparison

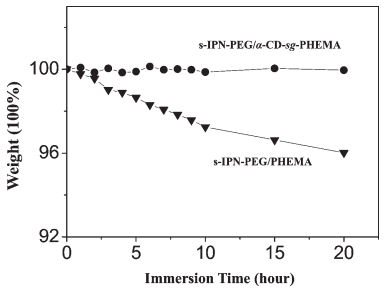

Figure 8. Weight loss of s-IPN-PEG/α-CD$_{1.1}$-*sg*-PHEMA$_{35}$ and s-IPN-PEG/PHEMA networks as a function of water immersion time.

to pristine PEG hydrogel, the little decrease in the tensile stress of sliding-ring PEG/(α-CD-BIBB)$_m$ hydrogels could be attributed to their relatively lower gel fraction (Table 1). A higher gel yield means a fewer defragments, leading to a higher tensile stress. The s-IPN-PEG/α-CD$_{1.1}$-*sg*-PHEMA$_{23}$ hydrogel has a tensile stress of about 980 kPa, which is much higher that of pristine PEG hydrogel. The increase in tensile stress of s-IPN-PEG/α-CD-*sg*-PHEMA may attribute to the entanglement, as well as the friction between the sliding-grafted PHEMA chains. The data in Table 1 also show that the longer the sliding-grafted PHEMA chains, the higher the tensile stress of s-IPN-PEG/α-CD-*sg*-PHEMA gels. It is obvious that the extension in the sliding-grafted PHEMA would enhance the entanglement. The maximum extension to break (MEB) of slide-ring PEG/(α-CD-BIBB)$_m$ and s-IPN-PEG/α-CD-*sg*-PHEMA hydrogels is lower than that of pristine PEG hydrogel. The data in Table 1 also reveals, the increase in the number of α-CD threaded onto PEG and the length of sliding-grafted PHEMA decreases the MEB. The PEG network form "click chemistry" is well-defined and the mesh size of networks is decided by the size of PEG. It is obvious, the bigger the mesh size, the larger space volume in the network lattices and thus a higher MEB. The introduction of the α-CD onto PEG lattice, as well as the sliding-grafted PHEMA chains would largely reduce the space volume among the lattice of PEG network, and thus leading to a low MEB.

3.4. Water Extraction. Hydrophilic semi-IPN is a good candidate for biomaterials.[54,55] However, the interpenetrating linear polymers, especially those with a relatively lower molecular weight would diffuse out from the semi-IPN. The diffusion of linear polymers from semi-IPN for a long time immersion in an aqueous solution, will not only reduce the physical and mechanical properties of semi-IPNs, but also limits their applications in biomedical fields.[37] To study the antiwater-extraction property of s-IPN-PEG/α-CD-*sg*-PHEMA hydrogel, a classical semi-IPN of PEG and PHEMA (s-IPN-PEG/PHEMA)was prepared under a same reaction condition as that of s-IPN-PEG/α-CD$_{1.1}$-*sg*-PHEMA$_{35}$, except using ethyl 2-bromobutyrate and N_3-PEG-N_3 instead of N_3-PEG-N_3/(a-CD-BIBB)$_m$ inclusion complex. Figure 8 shows the weight loss of s-IPN-PEG/α-CD$_{1.1}$-*sg*-PHEMA$_{35}$ and s-IPN-PEG/PHEMA hydrogels as a function of water immersion time. After 20 h water immersion, the weight of s-IPN-PEG/α-CD$_{1.1}$-*sg*-PHEMA$_{35}$ hydrogel was almost stable, while for s-IPN-PEG/PHEMA, the weight decreases to 96%. The weight loss of s-IPN-PEG/PHEMA could be attributed to the diffusion of the linear PHEMA from the s-IPN. Since the PHEMAs were fixed onto the network lattices, the diffusion of the PHEMAs from s-IPN-PEG/α-CD-*sg*-PHEMA hydrogels was largely prevented. The prolongation of the water extraction of s-IPN-PEG/PHEMA would cause a further weight loss due to the diffusion of PHEMA. However, after 48 h, the weigh loss was not as

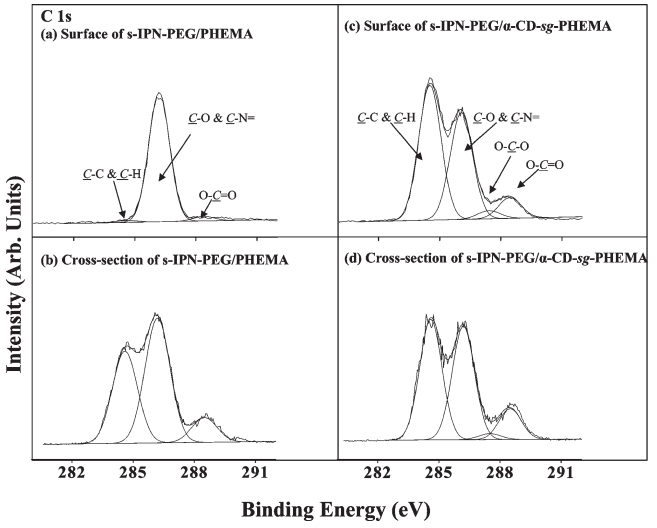

Figure 9. XPS C 1s core-level spectra of (a) of the surface of s-IPN-PEG/PHEMA, (b) of the cross-section of s-IPN-PEG/PHEMA, (c) of the surface of s-IPN-PEG/α-$CD_{1.1}$-*sg*-$PHEMA_{35}$, and (d) of the cross-section of s-IPN-PEG/α-$CD_{1.1}$-*sg*-$PHEMA_{35}$ networks after 20 h water immersion, respectively.

remarkable as the starting few hours, and maintained around of 6% after 72 h. The sol−gel fraction of s-IPN-PEG/α-CD-*sg*-PHEMA and s-IPN-PEG/PHEMA hydrogels can also be calculated from the data of SR and gel fraction of corresponding networks. The data in Table 1 shows the sol−gel fraction of s-IPN-PEG/α-CD-*sg*-PHEMA also maintained stable after water extraction, while the sol−gel fraction of the s-IPN-PEG/PHEMA changed from 2.7:6.3:91.0 ([PEG/α-CD]:[PHEMA]:[H_2O]) to 2.8:5.9:91.3.

The water extraction of s-IPN-PEG/α-CD-*sg*-PHEMA hydrogel was also studied by XPS measurements. Figure 9 shows the XPS C 1s core-level spectra (a) of the surface of s-IPN-PEG/PHEMA, (b) of the cross-section of s-IPN-PEG/PHEMA, (c) of the surface of s-IPN-PEG/α-$CD_{1.1}$-*sg*-$PHEMA_{35}$, and (d) of the cross-section of s-IPN-PEG/α-$CD_{1.1}$-*sg*-$PHEMA_{35}$ after 20 h water immersion, respectively. The spectrum of s-IPN-PEG/PHEMA can be curve-fitted into three peak components with bonding energy (BEs) at about 284.6, 286.2, and 288.4 eV, attributable to *C*−H/*C*−C, C−O/*C*−*N*= and O−*C*=O, respectively. Figure 9a has a very strong peak component at 286.2 eV, which is far from Figure 9b, but very similar to that of Figure 2a (pristine PEG network from CuAAC). The great difference in the chemical components between the surface and inside of s-IPN-PEG/PHEMA suggested, that 20 h of water immersion cause a large amount of the interpenetrating linear PHEMAs diffusing out from PEG networks. The spectrum of s-IPN-PEG/α-$CD_{1.1}$-*sg*-$PHEMA_{35}$ network can be curve-fitted into four peak components with bonding energy (BEs) at about 284.6, 286.2, 287.6, and 288.4 eV, attributable to *C*−H/*C*−C, C−O/*C*−N=, O−*C*−O and O−*C*=O, respectively. The similar spectra in Figure 9, parts c and d, suggest that after 20 h of water immersion, the s-IPN-PEG/α-CD-*sg*-PHEMA has a same chemical component both on surface and in bulks. XPS results suggest the s-IPN-PEG/α-CD-*sg*-PHEMAs exhibit a strong antiwater-extraction property, and the diffusion of interpenetrating linear polymers is largely prevented because the interpenetrating polymers are fixed on the network lattices.

4. Conclusions

A kind of novel semi-interpenetrating polymer networks (semi-IPN) with a unique molecular structure, poly(ethylene glycol) (PEG) network with movable sliding-graft poly(2-hydroxyethyl methacrylate) (PHEMA) brush (s-IPN-PEG/α-CD-*sg*-PHEMA), were successfully prepared by simultaneous "click chemistry" and atom transfer radical polymerization (ATRP). The number of the sliding-graft PHEMA can be regulated by threading different amount of α-CD-BIBB to N_3-PEG-N_3. The chain length of sliding-graft PHEMA can be tunable by changing the ATRP polymerization time. The s-IPN-PEG/α-CD-*sg*-PHEMAs exhibit a good physical and mechanical property. The s-IPN-PEG/α-CD-*sg*-PHEMAs hydrogels with various mechanical strengths were prepared by changing the molecular structure, such as the number and the chain length of sliding-graft polymer. Most important, the s-IPN-PEG/α-CD-*sg*-PHEMA hydrogels exhibit a strong antiwater-extraction. The diffusion of linear penetrating polymers from the networks under long time solvent immersion was largely prevented in s-IPN-PEG/α-CD-*sg*-PHEMA hydrogels, because the interpenetrating polymers were fixed on the network lattices. Furthermore, the sliding-graft polymers can afford the s-IPN-PEG/α-CD-*sg*-PHEMAs more functionalities, which extended their applications in biomedical fields. In summary, simultaneous "click chemistry" and ATRP is a powerful method to prepare semi-IPN with well-defined and designed molecular structures.

Acknowledgment. This work was supported by National Natural Science Foundation of China under the Grant 20804009 and 21074022, and the Key Project of Chinese Ministry of Education Grant 108062. This work was also supported by the Program for New Century Excellent Talents in University of Grant NCET-08-0117.

References and Notes

(1) Calvert, P. *Adv. Mater.* **2009**, *21*, 743–756.
(2) Myung, D.; Waters, D.; Wiseman, M.; Duhamel, P.; Noolandi, J.; Ta, C. N.; Frank, C. W. *Polym. Adv. Technol.* **2008**, *19*, 647–657.
(3) BajPai, A. K.; Shukla, S. K.; Bhanu, S.; Kankane, S. *Prog. Polym. Sci.* **2008**, *33*, 1088–1118.
(4) Jin, S. P.; Liu, M. Z.; Zhang, F.; Chen, S. L.; Niu, A. Z. *Polymer* **2006**, *47*, 1526–1532.
(5) Gitsov, I.; Zhu, C. *J. Am. Chem. Soc.* **2003**, *125*, 11228–11234.
(6) Reddy, T. T.; Kano, A.; Maruyama, A.; Hadano, M.; Takahara, A. *Biomacromolecules* **2008**, *9* (4), 1313–1321.
(7) Uzum, O. B.; Karadag, E. *J. Polym. Res.* **2007**, *14*, 483–488.
(8) Rasmussen, K.; Qstgaard, K. *Water Res.* **2003**, *37*, 519–524.
(9) Kopecek, J.; Yang, J. Y. *Polym. Int.* **2007**, *56*, 1078–1098.
(10) Ulijn, R. V.; Bibi, N.; Jayawarna, V.; Thornton, P. D.; Todd, S. J.; Mart, R. J.; Smith, A. M.; Gough, J. E. *Mater. Today* **2007**, *10*, 40–48.
(11) Chaterji, S.; Kwon, K.; Park, K. *Prog. Polym. Sci.* **2007**, *32*, 1083–1122.
(12) Lee, W.; Chen, Y. *J. Appl. Polym. Sci.* **2001**, *82*, 2487.
(13) Johnson, J. A.; Turro, N. J.; Koberstein, J. T.; Mark, J. E. *Prog. Polym. Sci.* **2010**, *35* (3), 332–337.
(14) Okumura, Y.; Ito, K. *Adv. Mater.* **2001**, *13*, 485–487.
(15) Ikeda, T.; Ooya, T.; Yui, N. *Macromol. Rapid Commun.* **2000**, *21*, 1257–1262.
(16) Fan, M. M.; Yu, Z. J.; Luo, H. Y.; Zhang, S.; Li, B. J. *Macromol. Rapid Commun.* **2009**, *30*, 897–903.
(17) Haraguchi, K.; Li, H. J. *Angew. Chem., Int. Ed.* **2005**, *44*, 6500–6504.
(18) Malkoch, M.; Vestberg, R.; Gupta, N.; Mespouille, L.; Dubois, P.; Mason, A. F.; Hedrick, J. L.; Liao, Q.; Frank, C. W.; Kingsbury, K.; Hawker, C. J. *Chem. Commun.* **2006**, *26*, 2774–2776.
(19) Crescenzi, V.; Cornelio, L.; Di Meo, C.; Nardecchia, S.; Lamanna, R. *Biomacromolecules* **2007**, *8*, 1844–1850.
(20) Ossipov, D. A.; Hilborn, J. *Macromolecules* **2006**, *39*, 1709–1718.
(21) Patten, T. E.; Matyjaszewski, K. *Adv. Mater.* **1998**, *10*, 901–915.
(22) Coessens, V.; Pintauer, T.; Matyjaszewski, K. *Prog. Polym. Sci.* **2001**, *26*, 337–377.
(23) Matyjaszewski, K.; Xia, J. *Chem. Rev.* **2001**, *101*, 2921–2290.
(24) Pyun, J.; Kowalewski, T.; Matyjaszewski, K. *Macromol. Rapid Commun.* **2003**, *24* (18), 1043–1059.
(25) Buathong, S.; Peruch, F.; Isel, F.; Lutz, P. J. *Design Monomer Polym.* **2004**, *7* (6), 583–601.

(26) Yu, Q.; Zeng, F.; Zhu, S. *Macromolecules* **2001**, *34*, 1612–1618.
(27) Mespouille, L.; Vachaudez, M.; Suriano, F.; Gerbaux, P.; Coulembier, O.; Degee, P.; Flammang, R.; Dubois, P. *Macromol. Rapid Commun.* **2007**, *28*, 2151–2158.
(28) Mantovani, G.; Ladmiral, V.; Tao, L.; Haddleton, D. M. *Chem. Commun.* **2005**, *16*, 2089–2091.
(29) Geng, J.; Lindqvist, J.; Mantovani, G.; Haddleton, D. M. *Angew. Chem., Int. Ed.* **2008**, *47*, 4180–4183.
(30) Xu, L. Q.; Yao, F.; Fu, G. D.; Shen, L. *Macromolecules* **2009**, *42*, 6385–6392.
(31) Xu, L. Q.; Yao, F.; Fu, G. D.; Kang, E. T. *Biomacromolecules* **2010**, *11*, 1810–1817.
(32) Liu, Z. Q.; Luo, Y. L.; Zhang, K. P. *J. Biomater. Sci., Polym. Ed.* **2008**, *19* (11), 1503–1520.
(33) Jin, S. P.; Liu, M. Z.; Chen, S. L.; Gao, C. M. *Eur. Polym. J.* **2008**, *44*, 2162–2170.
(34) Zhang, J.; Chu, L. Y.; Li, Y. K.; Lee, Y. M. *Polymer* **2007**, *48*, 1718–1728.
(35) Mohan, Y. M.; Geckeler, K. E. *React. Funct. Polym.* **2007**, *67*, 144–155.
(36) Sperling, L. H., *Interpenetrating Polymeric Networks and Related Materials*; Plenum Press: New York, 1981.
(37) Asoh, T.; Kaneko, T.; Matsusaki, M.; Akashi, M. *J. Controlled Release* **2006**, *110*, 387–394.
(38) Merrill, E. W.; Salzman, E. W.; Wan, S.; Mahmud, N.; Kushner, L. N.; Lindon, J.; Curme, J. *Am. Soc. Atrf. Intern. Organs* **1982**, *28*, 482–487.
(39) Whitesides, G. M.; Ostuni, E.; Takayama, S.; Jiang, X. Y.; Ingber, D. E. *Annu. Rev. Biomed. Eng.* **2001**, *3*, 335–373.
(40) *Biomaterials Science: An Introduction to Materials In Medicine*, 2nd ed.; Ratner, B. D.; Hoffman, A. S.; Schoen, F. J.; Lemons, J. E., Eds.; Elsevier Academic: Amsterdam, 2004.
(41) Li, J.; Loh, X. J. *Adv. Drug Deliv. Rev.* **2008**, *6*, 1000–1017.
(42) Yang, C.; Wang, X.; Li, H. Z.; Goh, S. H.; Li, J. *Biomacromolecules* **2007**, *8*, 3365–3374.
(43) Harada, A.; Kamachi, M. *Macromolecules* **1990**, *23*, 2821–2823.
(44) Araki, J.; Ito, K. *Soft. Matt.* **2007**, *3*, 1456–1473.
(45) Mayumi, K.; Ito, K. *Polymer* **2010**, *51*, 959–967.
(46) Zhao, C. M.; Domon, Y.; Okumura, Y.; Okabe, S.; Shibayama, M.; Ito, K. *J. Phys.: Condens. Matter* **2005**, *17*, S2841–S2846.
(47) Iyer, S. S.; Anderson, A. S.; Reed, S.; Swanson, B.; Schmidt, J. G. *Tetrahedron Lett.* **2004**, *45*, 4285–4288.
(48) Wei, H. L.; Zhang, A. Y.; Qian, L. J.; Yu, H. Q.; Hou, D. D.; Qiu, R. X.; Feng, Z. G. *J. Polym. Sci., Part A: Polym. Chem.* **2005**, *43*, 2941–2949.
(49) Wang, D. B.; Chen, B. H.; Yong, X. *Synth. React. Inorg., Met.-Org., Nano-Met. Chem.* **1997**, *27*, 479–486.
(50) Yu, H. Q.; Feng, Z G.; Zhang, A. Y.; Sun, L G.; Qian, L J. *Soft Matter* **2006**, *2*, 343–349.
(51) Lele, B. S.; Hoffman, A. S. *J. Controlled Release* **2000**, *69*, 237–248.
(52) Feng, Z. G.; Zhao, S. P. *Polymer* **2003**, *44*, 5177–5186.
(53) Beaumont, R. H.; Clegg, B.; Gee, G.; Herbert, J. B. M.; Marks, D. J.; Roberts, R. C.; Sims, D. *Polymer* **1966**, *7*, 401–417.
(54) Kwok, A. Y.; Qiao, G. G.; Solomom, D. H. *Chem. Mater.* **2004**, *16*, 5650–5658.
(55) Bajpai, A. K.; Shrivastava, M. *J. Biomater. Sci. Polym. Ed.* **2002**, *A39*, 237–256.